Comparison between two Algorithms based on different Wavelets to obtain the Planetary Boundary Layer height

Gregori de Arruda Moreira[a], Fábio J. da Silva Lopes[a], Juan Luis Guerrero-Rascado[b,c], Maria José Granados-Muñoz[b], Riad Bourayou[a], Eduardo Landulfo[a]

[a]Centro de Lasers e Aplicações (CLA) - Instituto de Pesquisas Energéticas e Nucleares (IPEN-CNEN), Av. Prof. Lineu Prestes 2242, Cidade Universitária, CEP 05508-000, São Paulo-SP, Brasil;

[b]Instituto de Astronomia, Geofísica e Ciências Atmosféricas (IAG) - Universidade de São Paulo (USP), Rua do Matão 1226, Cidade Universitária, CEP 05508-090, São Paulo-SP, Brasil;

[c]Instituto Interuniversitario de Investigación del Sistema Tierra en Andalucía (IISTA-CEAMA), Av. del Mediterráneo, 18006, Granada, España;

[d]Dpto. Física Aplicada, Universidad de Granada, Fuentenueva s/n, 18071, Granada, España;

ABSTRACT

Comprehension about the behavior of the Planet Boundary Layer (PBL) is an important factor in several fields, from analysis about air quality until modeling. However, monitoring the PBL evolution is a complex problem, because few instruments can provide continuous atmospheric measurements with enough spatial and temporal resolution. Inside this scenario lidar systems appear as an important tool, because it complies with all these capabilities- However, PBL observations are not a direct measure, being necessary to use complex mathematic algorithms. Recently, wavelet covariance transforms have been applied in this field.

The objective of this work is to compare the performing of distinct types of algorithms: a structured on Haar wavelet and other based on first derivative of Gaussian and Mexican Hat wavelets, and the results were compared with two Hysplit modelling. For this aim, two campaigns were carried out. From the results were possible to infer that both algorithms provide coherent results as the expected, but the Haar algorithm separates the sub-layers more efficiently, so it is the most appropriate to complex situations.

Keywords: lidar, Planetary Boundary Layer, Wavelet covariance transform, Haar, Mexican Hat, Hysplit.

1. INTRODUCTION

The Planetary Boundary Layer (PBL) is the region of troposphere, which feels the direct influence of forcing resulting from surface in interval time of one hour or less [1, 2]. The exchange of energy and momentum between the surface and atmosphere influences the PBL stability and it can increase or decrease it level of turbulence. Which can interfere in pollutants dispersion or imprisonment process in this layer. Because that, the studying about PBL became very important for a better understanding of how this process can influence the everyday life. [3].

The PBL height is an important variable and recurrently used in meteorology [2], from input data to models until mesoscale studies [3]. However, this parameter is not easy to derive it. One of the ways to get information about the PBL height is through radiossounding data, nevertheless this method usually has lower spatial and temporal resolution, not allowing to observe the PBL evolution due to the fact of radiosoundings are typically launched twice per day [4].

During the last decades, the use of the lidar technique (Light Detection And Ranging) to derive PBL heights application has grown substantially, and presenting promising results [4, 5, 6, 7, 8, 9, 10, 11, 12, 13, 14, 15, 16, 17, 18], since it has high spatial and temporal resolution, which enables to observe both qualitatively and quantitatively the PBL behavior.

Lidar Technologies, Techniques, and Measurements for Atmospheric Remote Sensing X,
edited by Upendra N. Singh, Gelsomina Pappalardo, Proc. of SPIE Vol. 9246, 92460D

However, monitoring the PBL behavior by lidar is not direct, being necessary to use algorithms to derive quantitative information of the PBL height [19]. Emeis et al. [9] presents a review about several algorithms that can be used to analyze lidar data, being the WCT (Wavelet Covariance Transform) one the most used [4, 5, 8, 10, 12, 13].

The aim of this study is to observe the behavior of two algorithms, the first based on Haar wavelet and the second one based on the First Derivative of Gaussian and Mexican Hat, analyzing the advantages and the disadvantages of both methods. Therefore, two measuring campaigns were carried out to obtain temporal evolution of PBL using Lidar system. The backscattered signals detected by it system were applied to the algorithms to derive the PBL heights and lately were compared between themselves and validated by Hysplit model.

2. METHODOLOGY

Two days of measurements were used in this study: 12th August 2013 and 29th April 2014 (Brazilians autumn and winter respectively, both during the dry season). Both measurements were conducted at same site, at IPEN (Nuclear and Energy Research) in São Paulo City (Brazil, Lat: 23.56°S and Long: 46.74°W) (Figure 1). For the first and second measurements were used a mobile (MSP-LIDAR II) and a fixed lidar system (MSP-LIDAR I) respectively, both operating with wavelength 532 nm. Both systems are part of LALINET (http://lalinet.org), which is a coordinated Lidar network focused on the vertically resolved monitoring of the particle optical properties distribution over Latin America.

Figure 1 – Location of IPEN (Nuclear and Energy Research Institute) where both lidar systems used in this study are installed.

2.1 Instrumentation

The MSP-LIDAR I is a 6-channel multiwavelengths coaxial system that uses a frequency-tripled Nd:YAG laser (Quantel model Brilliant-B) as the light source. It emits pulses energy of 400 mJ nominal at the 532 nm with a repetition rate of 10 Hz and pulse duration of 6 ns. The light beam is expanded by a factor of 5, in order to reduce the divergence of the expanded beam less than 0.5 mrad. The laser beam is vertically directed to the atmosphere and the backscatter radiation is collected with a Newtonian telescope that has a primary mirror diameter of 300 mm and a focal length of 1500 mm. The receiver field of view is set to 0.1 mrad, thus the complete overlap of laser beam and the telescope field of view is observed at altitudes higher than 500 m above the system, which limits the minimum range of our measurements. The detection box collects six different wavelengths and separates them into 6 different channels (the elastic 355 nm and the corresponding shifted Raman signals: nitrogen 387 nm, and water vapor, 408 nm; the elastic 532 nm and the corresponding shifted Raman signals: nitrogen 607 nm and water vapor 660 nm) using a combination of high-pass and low-pass filters. Each separated beam is directed to narrowbands spectral interference filters (532 ± 1 nm FWMH, 355 ± 1 nm FWMH, 387 ± 0.25nm FWMH, 408 ± 0.25 nm FWMH, 607 ± 0.25 nm FWMH, and 660 ± 0.25 nm FWMH) and then directed to photomultipliers tubes (PMTs). R7400 photomultiplier tubes from Hamamatsu are used for all channels,

except for 607 and 660 nm, where R9880U-20 are used. The R9880U-20 has a better quantum efficiency (around 20%) at range 550 - 700 nm, improving the signal to noise ratio of the weak Raman signal at theses wavelengths.

The MSP-LIDAR II is a biaxial mode single-wavelength backscatter Raymetrics LR101-V-D200. A frequency-doubled Nd:YAG laser (CFR200) is used as the light source. It emits pulses energy of 120 mJ nominal at the 532 nm with a repetition rate of 10 Hz and pulse duration of 9.2 ns. The light beam is expanded by a factor of 3, in order to reduce the divergence of the expanded beam less than 0.2 mrad. The laser beam is vertically directed to the atmosphere and the backscatter radiation is collected with a Cassegranian telescope that has a primary mirror diameter of 200 mm and a focal length of 800 mm. The receiver field of view is set to 1.25 mrad, thus the complete overlap of laser beam and the telescope field of view is observed at altitudes higher than 300 m above the Lidar system, which limits the minimum range of our measurements. After separating and passing the respective interference filters, the photons elastically backscattered at the 532 nm are detected with photomultiplier tube (PMTs, Hamamatsu – type R9880U-110), using a filter with bandwidth of 0.5 nm.

For both systems, a LICEL receiving electronics has provision to operate both in analog and photon counting mode and recording data 12-bit resolution. Data are averaged every 2 min, with a typical height resolution of 7.5 m.

2.2 The Wavelets

Wavelets are functions that enable to describe and decompound another function or data series, so that it is possible to analyze them in different time and frequency scales [20, 21, 22].

For the study about functions and/or series is used a method denominated Wavelet Transform, which consist on decomposition of the signal in several resolution levels. Thereby it is possible to perform an analysis from selected scale and to extract different information only changing the used "window" [4].

The Wavelet Transformations are subdivided in two groups: Continuous (CWT – Continuous Wavelet Transform) and Discrete (DWT – discrete Wavelet Transform), which are great tools to study temporal series, because they enable to decompound and filter them [21]. So, it is possible to conclude that the DWT can be used to study the atmospheric variables, because these has a temporal nature, being to it used the Wavelet Covariance Transform (WCT), which consists in detecting the changes in Range Corrected Signal (RCS) by the realization of a covariance of a Wavelet with the RCS. The WCT is given for the following equation:

$$WCT_{a,b}(r,t) = \sum_{r} P(r,t)\psi_{a,b}(r) \qquad (1)$$

where: $P(r,t)$ is the range corrected signal and $\psi_{a,b}(r)$ is the wavelet function. The latest must exhibit similar shape to the lidar signal. The PBL height will be the point where the $WCT_{a,b}(r,t)$ reaches its maximum value. In this study two algorithms are used and each one are structured on one distinct wavelet function.

2.2.1 Haar Wavelet (HW)

Baars et al. [5] and Brooks [6] suggest the utilization of Haar wavelet function in WCT algorithm. This function has a similar profile as the lidar signal, as can be observed in Figure 2. Haar function is given by the equation below:

$$h\left(\frac{z-b}{a}\right) = \begin{cases} -1: b - \frac{a}{2} \leq z \leq b \\ 1: b \leq z \leq b + \frac{a}{2} \\ 0: Other\ cases \end{cases} \qquad (2)$$

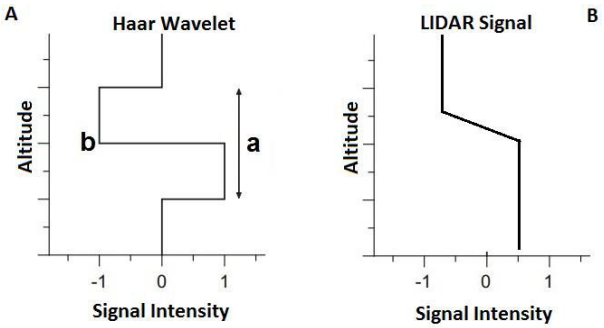

Figure 2: A –Haar wavelet. B – Lidar signal

The major difficulty to use this function is to choose ***a*** and ***b*** parameters [4, 5, 6], where the first represents the width of function and the second is the step selected. Moreira [4] proposes that ***a*** and ***b*** parameters must be chosen in accordance with different complexity levels of atmospheric conditions. In his study it was divide in three categories: stable (***a*** and ***b*** values do not to require a hard choose, but low values can provide detailed results), presence of multilayering (***a*** requires high values and ***b*** low values) and turbulent (***a*** needs high values and ***b*** requires approximately half of ***a*** value).

An important issue is the corrected separation among Convective Boundary Layer (CBL), Residual Layer (RL), Cloudy Layer (CL) and/or Aerosol Sublayer (AS). In order to solve this problem Brooks [5] uses a threshold technique to filter local maxima generated by RL, CL and AS, and, thus, CBL can be detected more easily. In this work it will be applied the threshold technique as well as the Brook's algorithm.

2.2.2 First Gaussian Derivative and Mexican Hat (FGDMH)

Another wavelet function that is often used in PBL height studies is the first Gaussian derivative. As can be seen in Figure 3, the wavelet has the same shape of lidar signal and it is satisfying the essential condition to overlay the covariance.

Morille et al. [13] uses two types of wavelets, the First derivative of a Gaussian and the Mexican Hat (Figure 2). The last one is used specifically to detect the aerosol and cloudy layers, solving the problem in separating CBL and others sublayers. The Mexican Hat Wavelet has similar shape of the discontinuity generated by the sublayers detected by the Lidar system. In opposite to the Haar function, the First Gaussian derivative is most often used to guarantee that all maxima lines propagate up to the finest scales [13]. By this way, is possible to accomplish the covariance in eq. 1, detect the presence of sublayers in the Lidar signal and extract the sublayer altitude from the Lidar profile.

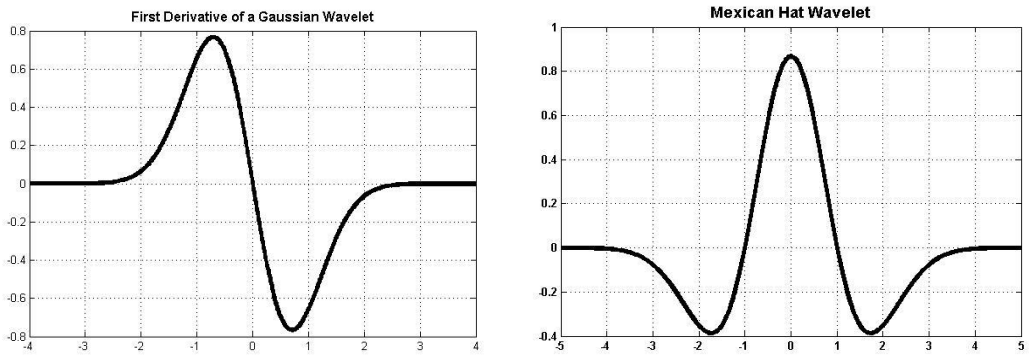

Figure 3 – First Derivative of a Gaussian Wavelet (Left) - Mexican Hat Wavelet (Right)

2.3 Hysplit

The Hybrid Single-Particle Langrangian Integrated Trajectory (HYSPLIT) model is a complete system for computing trajectories complex dispersion and deposition simulations [23]. In this study, HYSPLIT model was exclusively applied to obtain the PBL height, by means of two different methods: (i) Meteorological Model (MM) and (ii) Temperature Profile (TP) [23]. In (i) HYSPLIT calculates mixed layer depth value from a meteorological model, and in (ii) it computes the PBL altitude as the height at which the potential temperature is at least two degrees greater than the minimum potential temperature [23].

3. RESULTS AND DISCUSSION

3.1.1 – Day 12th August 2013

In this day the lidar measurements were performed from 09:21 to 17:47 (Local Time), with the MSP-LIDAR 2 operating at 532 nm. The Figure 4 shows the temporal evolution of the range corrected signal.

In Figure 4 it is possible to observe the ascension and decline of CBL, so these two periods can be clearly identified: Part I (where there is a fast CBL ascension) and Part II (covers the region where starts aerosol dilution until the end of afternoon, when the CBL starts to decline). In Part I, in a general way, the four methods provide similar results (Figure 5). For HW algorithm, the threshold technique using small values for **b** (Table 1), can minimize Residual Layer interference during the process of detection of CBL, showing a small overestimation respect to Hysplit computations (approximately 20%). The alternation of parameters in FGDMH does not influence significantly the shape of graphic FGDMH and it was not possible to do an effective separation between CBL and RL, showing a highly unexpected PBL heights and approaching to the results provided by other methods after 11:30 a.m. In Part II there is a great difference between Wavelet and Hysplit methods (on average higher than 400 meters). The HYSPLIT model indicates CBL decline starts at 15:00 hours, but the wavelets show that this phenomenon starts only after 17:00 hours.

When compared 2 by 2 throughout the whole measure time, the methods within the same class (from Hysplit or LIDAR data) show a correlation level (R^2) upper than 0.86, as can be seen in Figure 6. The wavelets show a R^2 value smaller than Hysplit parameterization, which can be justified by differences among rate growth. Figure 7 illustrates these variations throughout all measurement period. It is possible to observe that while HW shows a high growth rate (high values of slope – Table 2) in initial profile part and a strong decrease in final part, FDGMH displays less variations (low values of slope – Table 2), and with the exception Residual Layer stretch, this method provided values near Haar method.

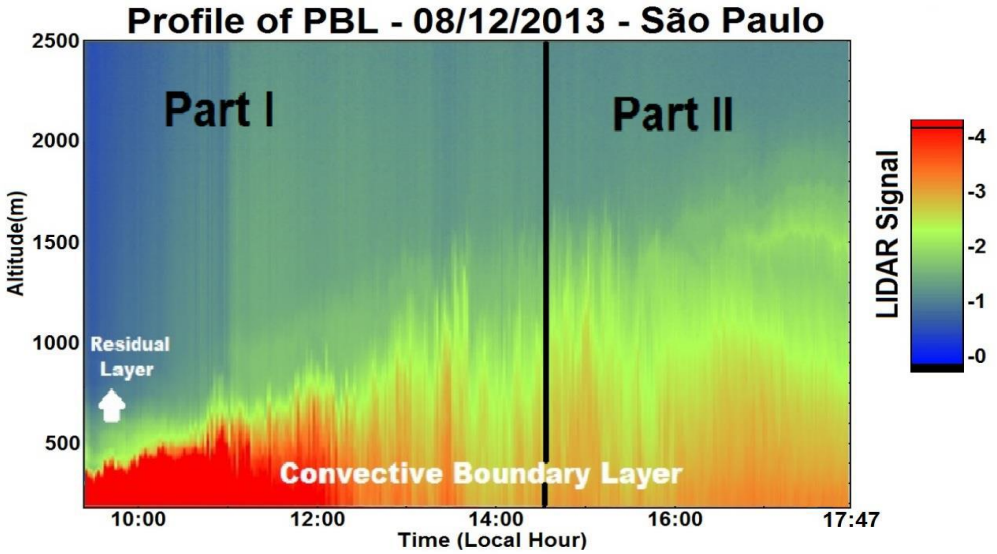

Figure 4 – Profile of PBL – 08/12/2013. Part I: Ascension of CBL (Left). Part II: Decline of CBL

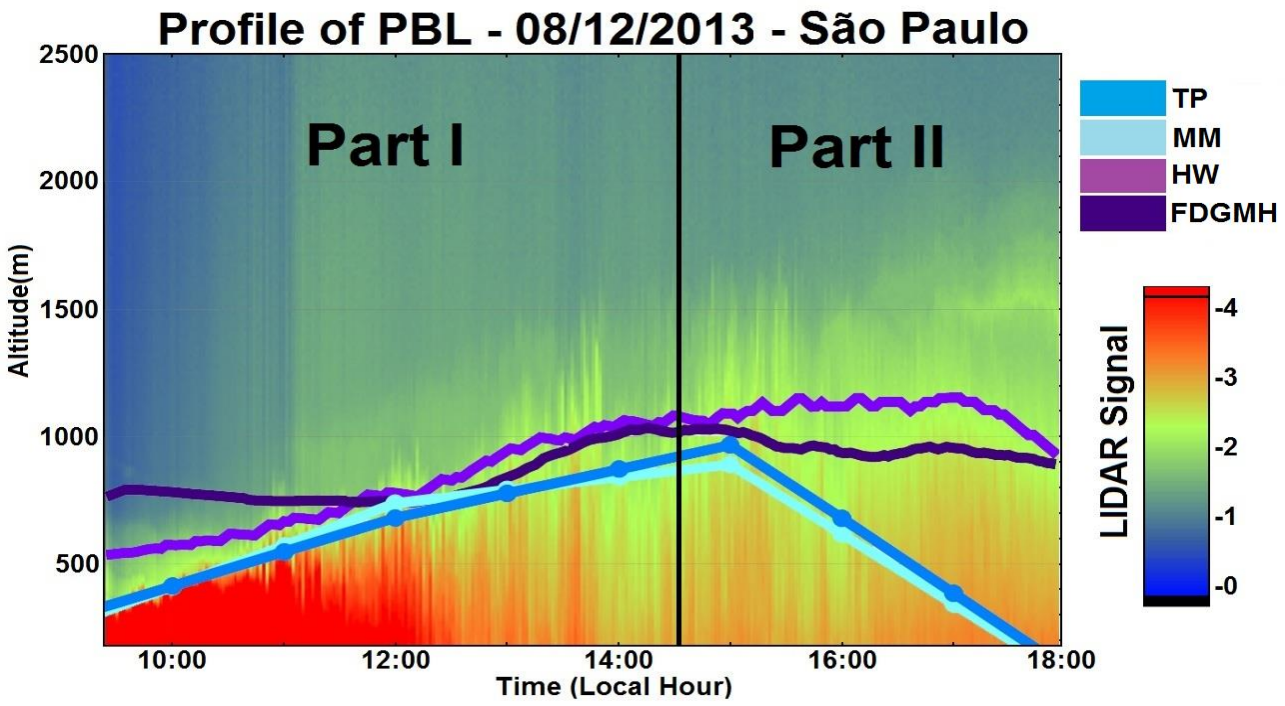

Figure 5 – Profile of PBL – Comparison among all methods.

Table 1 – Value of Parameters for WCT Methods

Algorithms	**Parameters**		**Threshold**	
HW	***a***	***b***		
	50	*10*	*0.2*	
FGDMW	**First Gaussian Derivate**		**Mexican Hat**	
	a	***b***	***a***	***b***
	100	*30*	*100*	*30*

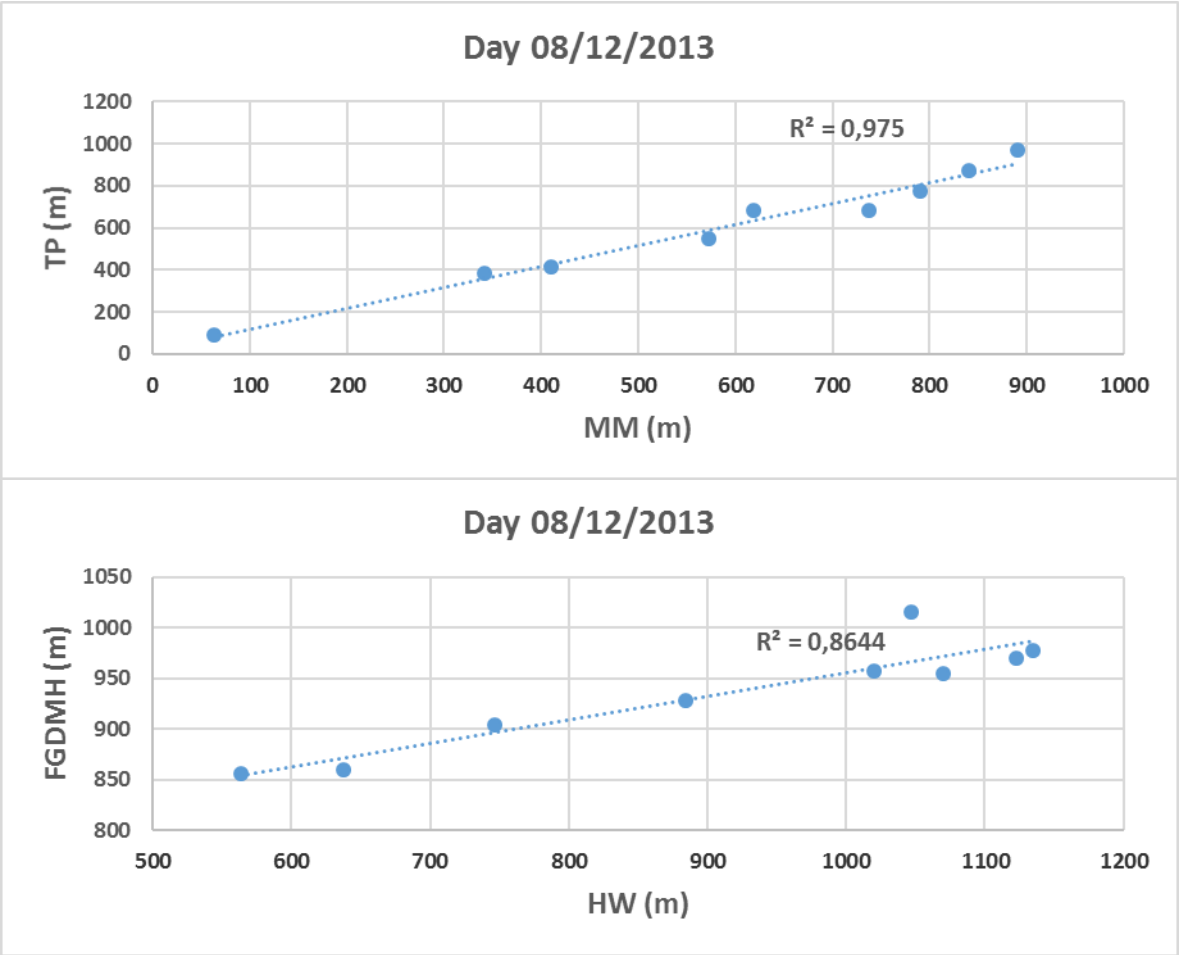

Figure 6 – Comparison between TKE and Mixing (upper). Comparison between Mexican Hat e Haar (lower)

In comparison with the computations obtained from HYSPLIT, both methods show a high correlation value (Table 2) in Part I, exhibiting good agreement among Modeling and Wavelets methods. For Part II, both methods have low correlation (Table 2), because premature modeling decline when they are compared as Wavelets.

Table 2 – Statistical Comparisons

Comparisons (x ; y)	Part I				Part II			
	R^2	Slope	Interceptions (m)		R^2	Slope	Interceptions (m)	
			x	y			x	y
(TP ; FGDMH)	*0.88*	*0.97*	*-95.60*	*92.70*	*0.51*	*-0.19*	*9424.30*	*1812.30*
(TP ; HW)	*0.95*	*2.31*	*556.40*	*-1283.90*	*0.13*	*-0.05*	*31262.93*	*1569.40*
(MM ; FGDMH)	*0.92*	*1.12*	*73.01*	*81.84*	*0.50*	*-0.24*	*7752.96*	*1835.90*
(MM ; HW)	*0.98*	*2.65*	*487.97*	*-1292.40*	*0.12*	*-0.06*	*25902.97*	*1574.90*

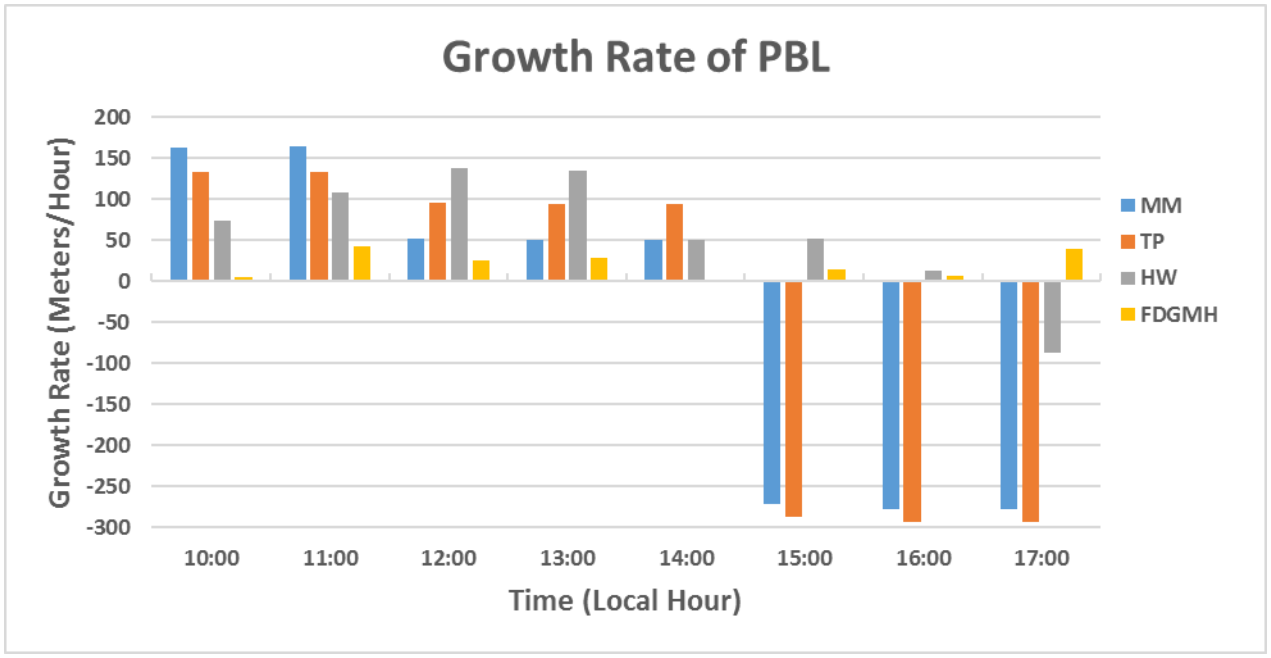

Figure 7 – Growth rate of PBL

The MM modelling has bigger correlation values than TP in part I, mainly for Haar, being R^2 nearly 1 (0.98). However in the Part II, as occurred in last comparison, both methods show low correlation, being it due to modeling indicate a CBL declining two hours before the wavelets.

3.1.2 – Day 12th August 2013

During this date, measurements were carried out using the MSP-LIDAR II system with 532 nm wavelength, starting at 09:34 and finishing at 16:57 (Local time).

For this case the analysis was divided in two parts: Part I (since the beginning of measurement until 13:00, containing a fast growth of CBL) and Part II (it covers the region where CBL has a slow growth and it starts to decline), as can be seen in Figure 8.

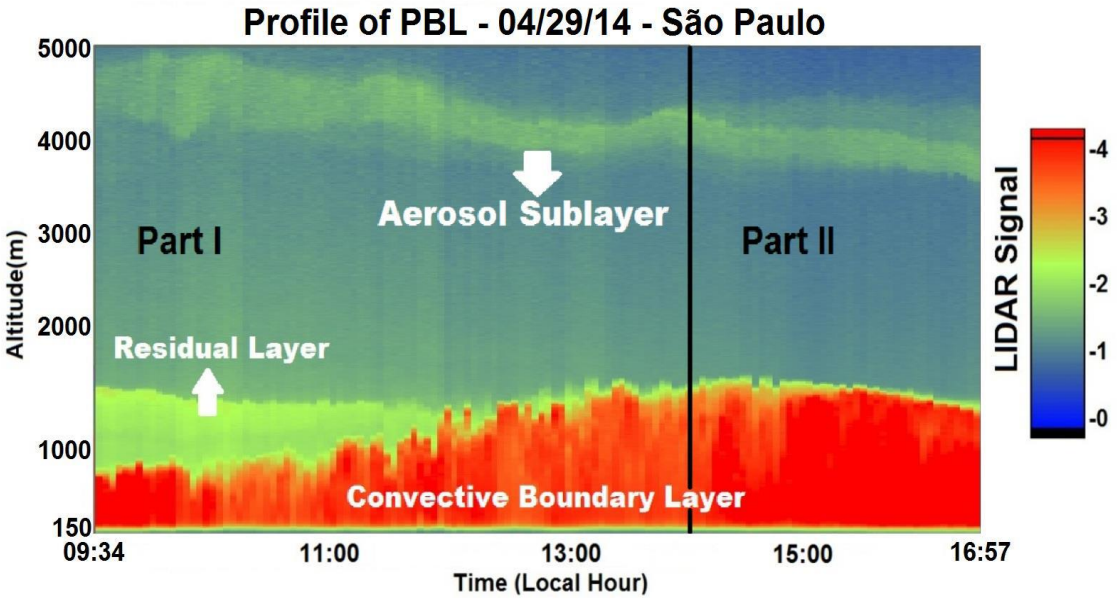

Figure 8 – Profile of ABL – 04/29/2014 Part I: Ascension of CBL (Left). Part II: Decline of CBL (Right)

Figure 9 exhibits a comparison among the four methods used, and by it is possible to observe that methods from HYSPLIT has behavior similar to Wavelets in Part I, but in Part II occur a detachment among them, due to the modeling decline precociously around at 15:00.

The methods obtained from HYSPLIT has a high level of correlation each other (R^2 = 0.99 – Figure 10) and consequently similar growth rate (Figure 11) throughout all profile. The Wavelets also has considerable correlation rate (R^2 = 0.82 – Figure 10), but this is smaller than that showed in before situation. This can be attributed at high complexity of this day, which although has a well-defined CBL, it has too a thick Residual layer and it endures a long time, since this point where there is the bigger difference between the CBL growth rate (Figure 11). This difficult parameters and threshold chose for HW, being that many combinations were used but was not possible to separate totally the Residual Layer interference even using a high threshold values (Table 3), so that the FGDMH algorithm has too a hard parameters chose, but it get to separate the Residual Layer of CBL. In final part of profile, although the methods indicate the decline of CBL from different heights, both show similar growth rate, since equals in last point (Figure 11).

Table 3 – Value of parameters for WCT Methods

Algorithms	**Parameters**		**Threshold**	
HW	***a***	***b***		
	150	*20*	*0.8*	
FGDMH	**First Gaussian Derivate**		**Mexican Hat**	
	a	***b***	***a***	***b***
	100	*30*	*100*	*30*

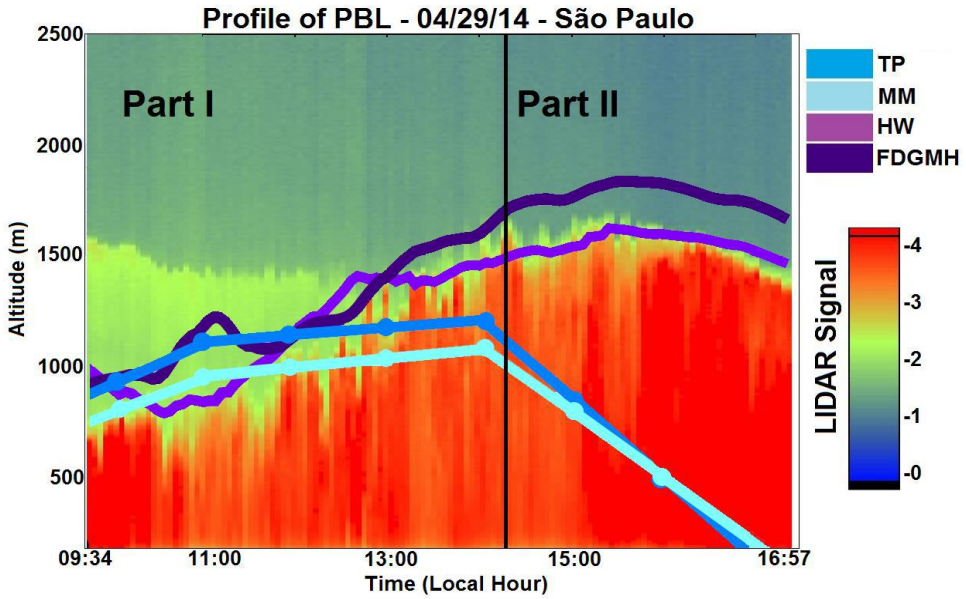

Figure 9 – Profile of PBL – Comparison among all methods

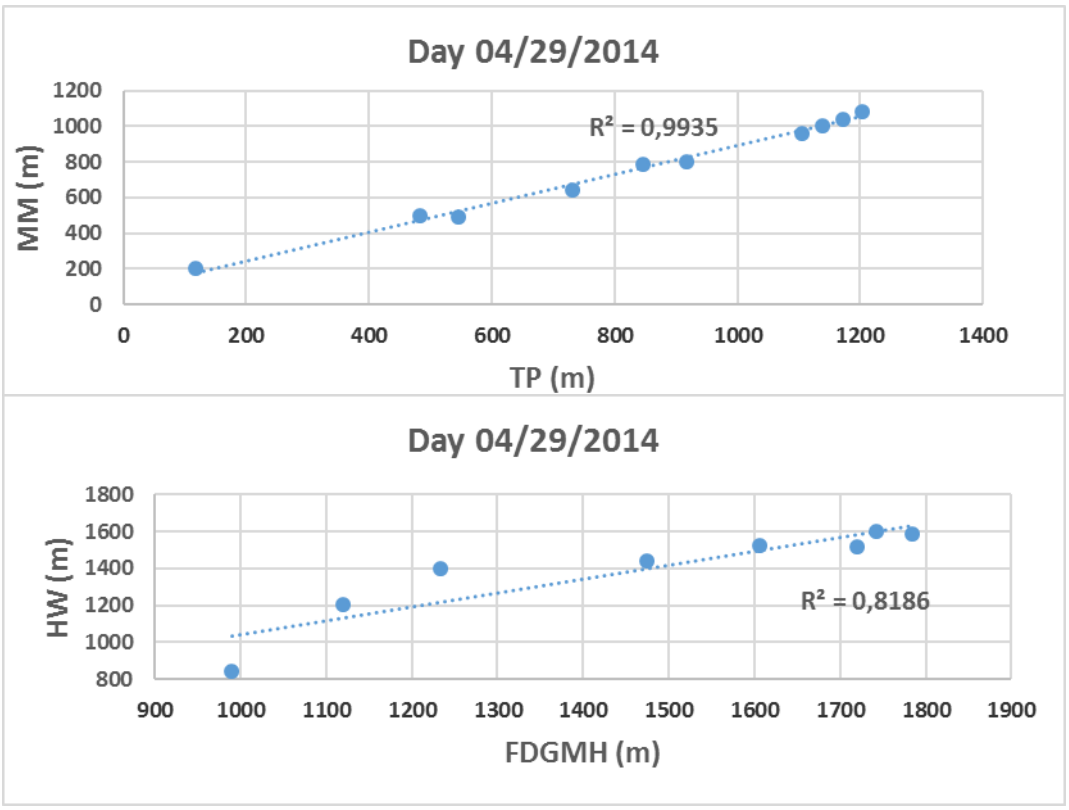

Figure 10 - Comparison between TP and MM (upper). Comparison between FDGMH e HW (lower)

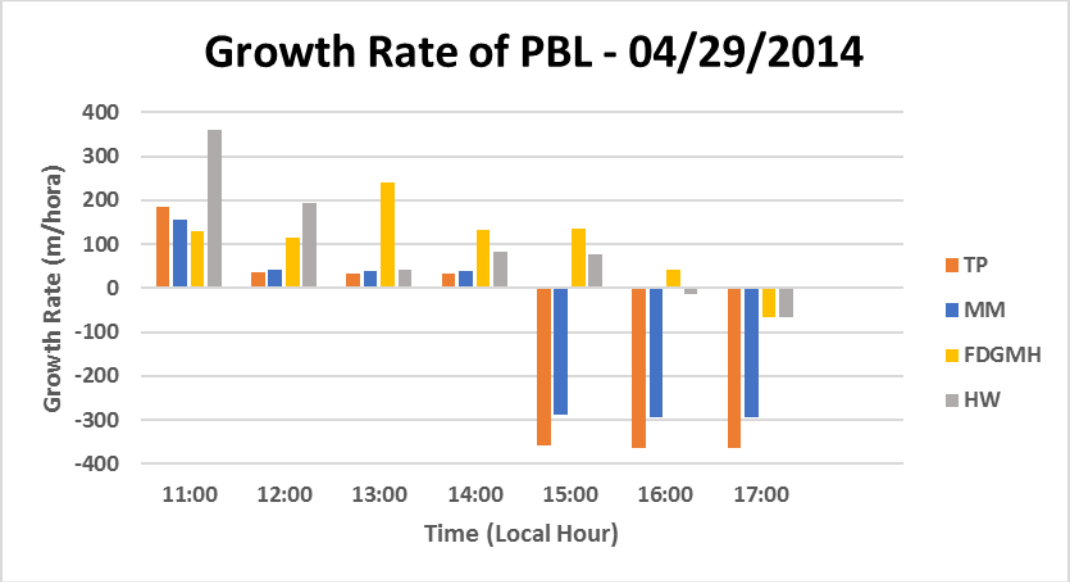

Figure 11 – Growth rate of PBL

In comparison with TP parameterization, both methods has high correlation rate for Part I and low correlations in Part II (Table 4). This occur because in Part I TP and Wavelets methods have same signal of Growth rate (Figure 11), but in Part II the signals of them became different.

Table 4 – Statistical Comparisons

Comparisons (x ; y)	Part I				Part II			
	R^2	Slope	Interceptions (m)		R^2	Slope	Interceptions (m)	
			x	y			x	y
(TP ; FDGMH)	*0.95*	*0.23*	*3197.77*	*747.32*	*0.55*	*-0.06*	*-15720.93*	*1014.00*
(TP ; HW)	*0.96*	*0.99*	*116,80*	*116.11*	*0.03*	*0.02*	*54979.70*	*1083.10*
(MM ; FDGMH)	*0.86*	*0.23*	*3224.44*	*746.87*	*0.50*	*-0.06*	*14844.57*	*1012.40*
(MM ; HW)	*0.86*	*0.23*	*3112.26*	*723.60*	*0.03*	*0.02*	*52096.15*	*1083.60*

The MM also has a high correlation with Wavelets methods (Table 4) in Part I. But in Part II, as well as occurred in other cases, the correlation levels are low, being it too observed in Fig. 11, where there is a big difference among growth rate of Wavelet methods (at beginning positive and posteriorly negative) and MM, which are negatives along of Part II, because the decrease indicated from 14:00.

4. CONCLUSIONS

The use of Wavelets provides a detailed and high quality analyze of digital signals. This job objectified to realize a comparison between two different methods based in covariance between wavelets and LIDAR signal, being this methods HM, which uses Haar wavelet, and FDGMH, who combine two wavelets: the first derivative of Gaussian function and

Mexican Hat. Both methods were compared with two types of parameterizations from HYSPLIT model in two days of measurement.

When compared each other, the methods from lidar data shown a high level of correlation along time of measure ($R^2 \geq 0.82$). For cases when the atmosphere has a simple profile (08/12/2013), the correlation values are greater than those compared with more complex days (04/29/2014). Because the presence of aerosol and cloudy sublayers and/or residual layer can interfere in results, so each methods has it particular characteristic to separate the CBL of others layers. In comparison with HW, FDGMH did theses separation more efficiently.

In comparison with HYSPLIT model, the wavelets methods exhibited a considerable coherence level ($R^2 \geq 0.85$) during CBL ascension. Nevertheless, when CBL rate growth starts to decline and it stabilizes itself, because aerosol concentration begins to decrease due to dilution, the correlation shown low levels (Table 2 and 4), because in this part HYSPLIT and Wavelets disagree in growth rate.

Although there are discrepancies in some regions of the PBL profile, the methods based on wavelets used in this study show a good correlation and they can describe the PBL evolution in some degree of confidence. The Haar Wavelet has good agreement with the modeling and it is the more appropriate to be used applied, and the Haar Wavelet method reaches R^2 values bigger than the FDGMH.

In future studies are planned to do similar approaches with other meteorological models and experimental methods of PBL detection and with more variable atmospheric situations.

Acknowledgments

This work was supported by Nuclear and Energy Research Institute (IPEN), FAPESP (Fundação da Amparo à Pesquisa do Estado de São Paulo) through the Posdoctoral project 2011/14365-5 and the thematic project 2008/58104-8; in a collaboration between the Institute of Astronomy, Geophysics and Atmospheric Sciences (IAG) of the University of São Paulo (USP) and, and by the University of Granada through the contract \Plan Propio. Programa 9. Convocatoria 2013". The authors would like to acknowledge the Center for Lasers and Applications for supporting the project.

REFERENCES

[1] Garratt, J. R. The Atmospheric Boundary Layer. Cambridge University Press, 1992.

[2] Stull, R. B. An Introduction to Boundary Layer Meteorology. Kluwer Academic Publishers, 1988.

[3] Wallace, J. M., and Hobbs, P. V. Atmospheric Science - An Introductory Survey. Academic Press, 2006.

[4] Moreira, G. de Arruda – Métodos para obtenção da altura da Camada Limite Planetária a partir de dados de LIDAR. 2013. 126f. Master's degree dissertation – Universidade de São Paulo. 2013.

[5] Baars, H., Ansmann, A., Engelmann, R., and Althausen, D. Continuous monitoring of the boundary-layer top with lidar. Atmospheric Chemistry and Physics 8 (2008), 7281 -7296.

[6] Brooks, I. M. Finding boundary layer top: Application of a wavelet covariance transform to lidar backscatter proles. Journal of Atmospheric And OceanicTechnology 20 (2003), 1092-1105.

[7] Cohn, S. A., and Angevine, W. M. Boundary layer height and entrainment zone thickness measured by lidars and wind-proling radars. Journal of Applied Meteorology 39 (2000'), 1233-1247.

[8] Davis, K. J., Gamage, N., Hagelberg, C. R., and Kielme, C. An objective method for deriving atmospheric structure from airbone lidar observations. Journal of Atmospheric And Oceanic Technology 17 (2000), 1451 - 1468.

[9] Emeis, S., Schäfer, K., and Münkel, C. Surface-based remote sensing of the mixing - layer height - a review. Meteorologische Zeitschrift 17 (2008), 621- 630.

[10] Granados-Muñoz, M. J., Navas-Guzmán, F., Bravo-Aranda, J. A., Guerrero-Rascado, J. L., Lyamani, H., Fernandez-Galvez, J., and Arboledas, L. A. Automatic determination of planetary boundary layer heights using lidar: One-year analysis over southeastern Spain. Journal of Geophysical Research 117(2012).

[11] Menut, L., Flamant, C., Pelon, J., and Flamant, P. H. Urban boundary-layer height determination from lidar measurements over the paris area. Applied Oprtics 38 (1999), 945 - 954.

[12] Moreira, G. A., Bourayou, R., Lopes, F. J. da S., Albuquerque, T. A, Reis Jr, N. C., Held, G., Landulfo, E. "Automatic methods to detect the top of atmospheric boundary layer", in Lidar Technologies, Techniques, and Measurements for Atmospheric Remote Sensing IX, Upendra N. Singh; Gelsomina Pappalardo, Editors, Proceedings of SPIE Vol. 8894 (SPIE, Bellingham, WA 2013), 88940T.

[13] Morille, Y., Haeffelin M., Drobinski, P. and Pelon, J. STRAT: An Automated Algorithm to Retrieve the Vertical Structure of the Single-Channel LIDAR Data. Journal of Atmospheric and Oceanic Technology 24 (2007), 761 – 775.

[14] Seibert, P., Beyrich, F., Gryning, S.-E., Joffre, S., Rasmussen, A., and Tercier, P. Review and intercomparison of operational methods for the determination of the mixing height. Atmospheric Environment 34 (2000), 1001 - 1027.

[15] Steyn, D. G., Baldi, M., and Hoff, R. M. The detection of mixed layer depth and entrainment zone thickness from lidar backscatter proles. Journal of Atmospheric and Oceanic Technology 16 (1999), 953 - 959.

[16] Talianu, C., Nicolae, D., Ciuciu, J., Ciobanu, M., and Babin, V. Planetary boundary layer height detection from lidar measurements. Journal of Optoelectronics and Advanced Materials 8 (2006), 243 - 246.

[17] Tomasi, F. D., and Perrone, M. R. PBL and dust layer seasonal evolution by lidar and radiosounding measurements over a peninsular site. Atmospheric Research 80 (2006), 86 - 103.

[18] Vickers, D., and Mahrt, L. Evaluating formulations of stable boundary layer height. Journal of Applied Meteorology 43 (2004), 1736 - 1749.

[19] Kovalev, V. A., and Eichinger, W. E. Elastic LIDAR - Theory, Practice and Analysis Methods. John Wiley & Sons, 2004.

[20] Addison, P. S. Wavelet transforms and the ecg: A review. Physiological Measurement 26 (2005), 155-199.

[21] de Oliveira, Hélio Magalhães. Análise de Sinais para Engenheiros: Uma abordagem via Wavelets. 1 ed. [S.l.]: BRASPORT, 2007. 268 p. ISBN 9788574522838

[22] Vilani, M. T. Análise de Fourier e Wavelet em Variáveis Micrometeorológicas em Diferentes Tipologias de Ocupação. PhD thesis, Universidade Federal de Mato Grosso, 2011.

[23] R. R. Draxler and G. D. Hess, “An overview of the HYSPLIT 4 modeling system of trajectories, dispersion, and deposition,” Australian Meteorological Magazine 47, pp. 295–308, 1998